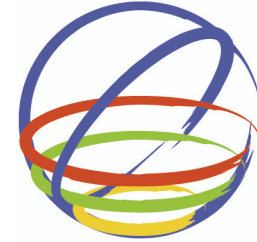


Effect of Bearing Behaviour on the Response of Anchored Equipment in Seismically Isolated Buildings



Konstantinidis, Dimitrios

McMaster University, Hamilton, Canada

Yang, T.Y.

University of British Columbia, Vancouver, Canada

Kelly, James M.

University of California, Berkeley, USA

SUMMARY

The seismic isolation code used in the United States is conservative in many of its provisions. For static analysis and for the selection of time histories, the spectrum is constant-velocity for periods over one second, leading to large displacements for long-period systems. The damping systems used to reduce these displacements are hysteretic with the characteristic that damping decreases with increasing displacement. The damping necessary to control displacements for a very rare seismic event is very large under more realistic levels of seismic input, resulting in stiffening of the isolation system and substantial reduction in the efficiency of the isolation. This in turn has a negative impact on acceleration-sensitive internal equipment. This paper suggests an alternative approach that conforms to code requirements and ensures that, at moderate earthquake inputs, the equipment remains protected, and the large code-mandated displacements are kept to acceptable levels.

Keywords: damping, hysteresis, equipment, base isolation, vibration isolation

1. INTRODUCTION

The fact that the seismic isolation code which must be used for all seismic isolated buildings in the United States is very conservative has been pointed out by many authors, among them Mayes (2002) and Naaseh et al. (2004). As a consequence of this conservatism, seismic isolation while flourishing in other countries, is underused in the US. The main source of the conservatism in all versions of the US code for seismic isolated structures is the default response spectrum. For static analysis and for the construction of time histories, the target spectrum is a constant velocity spectrum from periods around one second and longer. This type of spectrum leads to large displacements for long period systems and pushes the designer of the system to use high damping in an attempt to reduce these displacements; this in turn reduces the effectiveness of the isolation system. If the default spectrum were to reflect real ground motions, it would become a constant displacement spectrum at a period of around two seconds. There would be an incentive to use longer period systems and take advantage of the reduction in base shear that for a constant displacement spectrum decreases with the square of the period.

The basic problem with the design approach in the current code is that isolation systems are used mainly for buildings that house sensitive and expensive internal equipment. The conservatism in the design process makes it uneconomic to use isolation for the protection of the structural system itself. The design base shear for an isolated superstructure exceeds that for the equivalent fixed-base structure. Thus typical examples of base isolated buildings are emergency service centers, hospitals, chip fabrication factories and similar structures where the internal equipment is much more important than the structure. The damping systems that are available to control the large displacements that come from the conservatism in the code are hysteretic such as metallic yielding, friction or low exponent viscous dampers. All of these systems have the characteristic that the damping is strongly displacement-dependant. To achieve the level of damping to reduce the code-mandated displacements at the Maximum Considered Earthquake (MCE) hazard level means that at lower shaking intensity (which represents a more realistic level of seismic input that might be experienced over the working

life of the building), the system will have higher damping and stiffness (since the displacement of the isolator decreases), and therefore the building may not act as an isolated one. In this case, there may be serious damage to the sensitive internal equipment.

It is worth noting that although the code permits the use of high damping in the isolation system to reduce the design displacement, only the elastic force is included in the calculation of the base shear. At 50% damping, which has the highest reduction factor permitted in the IBC2000 code (ICC 2000), the damping force is the same as the elastic force. This provides the incentive for the use of highly damped systems, but damping, even linear viscous, but especially nonlinear hysteretic damping, amplifies response in the higher modes of the isolated structure that in turn produces higher floor accelerations which can cause damage in the equipment.

The purpose of this paper is to show how highly damped isolation systems are counterproductive to the main purpose of isolation and to suggest an alternative approach to the design of isolation systems which is based on a property of natural rubber called strain-induced crystallization. This design approach will still conform to the code requirements for Design Based Earthquake (DBE) level of superstructure base shear and MCE level of displacement but also ensure that at low or moderate seismic shaking, the equipment remains protected, and the large code-mandated displacements are kept to acceptable levels.

2. CURRENT CODE REQUIREMENTS

The seismic isolation code in the US requires the calculation of two displacement quantities denoted by D_M and D_D from which all other design quantities are determined. The first is important for the design and testing of the isolation system and the second for the design of the superstructure:

$$D_M = \frac{g}{4\pi^2} \frac{S_{M1} T_M}{B_M}, \quad D_D = \frac{g}{4\pi^2} \frac{S_{D1} T_D}{B_D} \quad (2.1)$$

where g is the gravitational acceleration; S_{M1} is the MCE 5% damped spectral acceleration at 1-sec period; T_M is the effective period (in seconds) of the seismic isolated structure; B_M is the damping reduction factor which depends on the equivalent viscous damping ratio as shown in Table 1, which is offered in the code and reproduced here for convenience; S_{D1} is 2/3 of S_{M1} , and T_D and B_D are the period and damping reduction factor for the displacement D_D .

Table 1. Damping reduction factor

Equivalent viscous damping ratio, β_{eff}	B_M or B_D
$\leq 2\%$	0.8
5%	1.0
10%	1.2
20%	1.5
30%	1.7
40%	1.9
$\geq 50\%$	2.0

(2.2)

The unreduced base shear is calculated from D_D multiplied by the system stiffness and reduced by a reduction factor R_f which is 3/8 of the R -value for a fixed-base structure of the same kind, not to exceed 2. Engineers rely on using damping to reduce D_D , which in turn reduces the design base shear.

3. BILINEAR HYSTERETIC BEHAVIOUR OF TYPICAL ISOLATORS

The two models to be designed are either the Lead Plug System (LPS) or the Friction Pendulum System (FPS), both of which are usually represented by bilinear models. This model is fully characterized by three parameters: the characteristic strength Q , the second stiffness K_2 , and the yield

displacement D_y , shown in Fig. 1 (left). In terms of these parameters and the generic displacement, D , three important quantities are derived: the initial stiffness, K_1 , the effective stiffness, K_{eff} , and the effective damping, β_{eff} , as shown on the right of Fig. 1.

In the case of LPS, the K_1/K_2 ratio is generally taken to be around 10 (Skinner et al. 1993), while for the FPS it is taken to be around 100. Since both D and β_{eff} are dependent on the initially unknown D , it is necessary to use an iterative procedure to calculate D . Another useful quantity to define is the energy dissipated per cycle given by $W_D = 4Q(D - D_y)$, which for an equivalent viscously damped linear oscillator with stiffness K_{eff} and damping ratio β_{eff} is

$$W_D = 4Q(D - D_y) = 2\pi\beta_{eff}K_{eff}D^2 \quad (3.1)$$

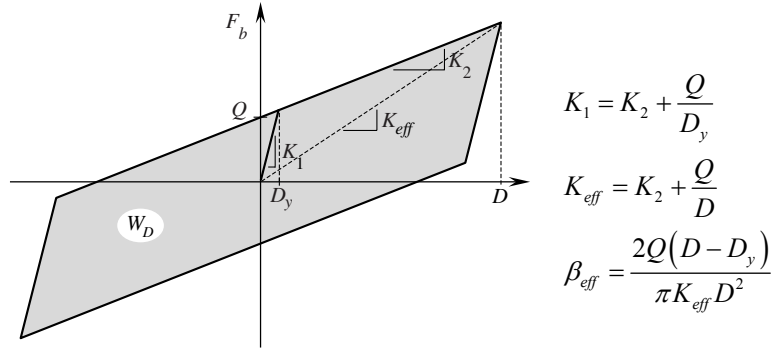


Figure 1. Bilinear hysteretic behaviour of isolator

4. SELECTION AND SCALING OF THE GROUND MOTIONS

This study examines the response of a seismic-isolated building subjected to earthquake motions from three seismic hazard levels: (1) Maximum Considered Earthquake (MCE), adopted in the code to represent very rare earthquakes; (2) Design Based Earthquake (DBE), adopted in the code to represent rare earthquakes; and (3) Service Level Earthquake (SLE), which is selected by the authors to represent moderate earthquake events that are more likely to occur over the lifetime of the building. The spectral acceleration of SLE is chosen by the authors to be 1/2 of DBE. This is not intended to represent any particular return period or probability of occurrence but merely to be the basis for an assessment of the impact of damping on the floor accelerations and interstory drifts at earthquake levels below those of the code. The scaling factor choice of 1/2 is also made by Marriott et al. (2008).

The figure on the right of Table 2 shows the DBE spectrum (heavy black line) for a prototype building located in downtown Berkeley, on Soil Type C. The spectrum was calculated using IBC2000 (ICC 2000), with $S_s = 2.1$, $S_1 = 0.94$, and $S_{D_s} = 1.4$, $S_{D_1} = 0.82$. Table 2 (shows) shows the ground motions selected for time history analysis. The ground motions were amplitude-scaled to best match the DBE spectrum in the period range from $0.5T$ to $1.25T$ (where $T = 2.50$ sec for this prototype building). The scaling factors are listed in Table 2, and the figure to the right shows the scaled response spectra. To obtain the MCE and SLE seismic hazard level motions, the scaled ground motions (DBE level) were scaled further by a factor of 1.5 and 0.5, respectively.

5. DESIGN OF LEAD PLUG SYSTEM

To study the effect of the isolation hysteresis on the building and equipment performance, an LPS was designed according to IBC2000 (ICC 2000). We begin with the premise that a linear 5% damped system with 2.50 sec period will produce a maximum displacement of 30.0 in. at the MCE hazard level. The designer feels that this must be reduced by the use of damping. For 20% equivalent viscous damping, Table 1 gives $B_M = 1.5$, which reduces the MCE displacement D_M to 20.0 in. Suppose that

the carried load is W and that the period is unchanged at 2.50 sec, then the effective stiffness is $K_{eff} = (2\pi/T)^2 W/g = 0.0164W/\text{in.}$, and the energy dissipated per cycle is $W_D = 2\pi\beta_{eff}K_{eff}D^2 = 2\pi(0.20)(0.0164W)(20.0)^2 = 8.23W \cdot \text{in.}$ From these, the first estimate of the characteristic strength of the isolation system is calculated by assuming the yield displacement equals zero, giving $Q = W_D/[4(D - D_y)] = 0.103W$, and the second stiffness of the isolation system is $K_2 = K_{eff} - Q/D = 0.0113W/\text{in.}$ The yield displacement is $D_y = Q/(K_1 - K_2) = 1.01 \text{ in.}$, where $K_1 = 10K_2$. Substituting the calculated D_y into the above equations and repeating the process a few times, the properties of the LPS converge to

$$Q = 0.109W; \quad K_2 = 0.0109 \frac{W}{\text{in.}}; \quad D_y = 1.11 \text{ in.} \quad (5.1)$$

The resulting load-displacement curve for the LPS is shown in Fig. 2. Once the LPS is designed for the MCE, the performance of the building and equipment under lower earthquake shaking intensities is studied. For example, when the earthquake shaking intensities is reduced to DBE, the S_{D1} is $2S_{M1}/3 = 0.82$. If we start by assuming that the period is still 2.50 sec, and the damping is 20%, then D_D is 13.3 in. For this displacement, the effective stiffness is $K_{eff} = K_2 + Q/D = 0.0191W/\text{in.}$ The corrected period and effective damping are

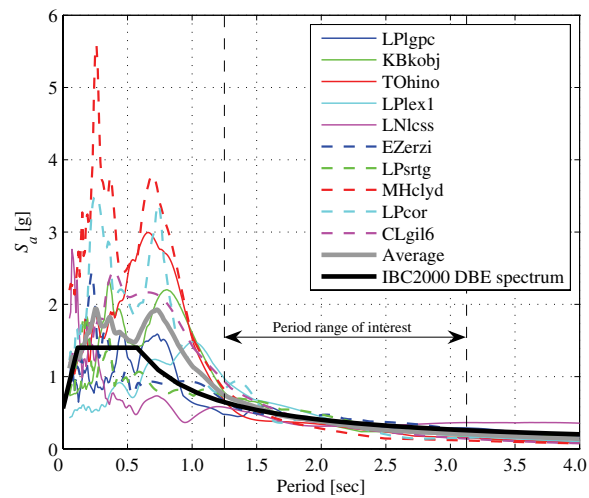
$$T = 2\pi \sqrt{\frac{W}{K_{eff}g}} = 2.31 \text{ sec}, \quad \beta_{eff} = \frac{4Q(D - D_y)}{2\pi K_{eff}D^2} = \frac{4(0.109W)(13.3 - 1.11)}{2\pi(0.0191W)(13.3)^2} = 0.250 \quad (5.2)$$

which gives a damping reduction factor $B_D = 1.60$ (Table 1) and produces a new estimate displacement D_D of 11.6 in. Substituting D_D in the above equations, and after a few iterations, $D = 10.6 \text{ in.}$, $T = 2.20 \text{ sec}$, and $\beta_{eff} = 27.6\%$ at the DBE seismic hazard input.

When the input is reduced to the SLE level (i.e., $S_{S1} = S_{M1}/3 = 0.41$), the same iterative approach provides a period of 1.58 sec, a damping of 32.4% and a displacement of 3.6 inches. It is clear that the influence of the hysteretic damping on the response, at least that calculated from the code formulas, is affected both by increased damping as the input decreases but also from the shortening of the period. As the input is decreased by a factor of three, the displacement response is decreased by a factor of five.

Table 2. Ground motions used in this study

Earthquake/Station	Record Name	Scale Factor
Coyote Lake, CA, 1979/6/8 Gilroy # 6	CLgil6	0.70
Landers, CA, 1992/6/28 Lucerne Valley	LNlcss	0.85
Morgan Hill, CA, 1984/4/24 Coyote Lake Dam	MHclyd	0.85
Loma Prieta, CA, 1989/10/17 Los Gatos Pres. Cntr	LPlgpc	0.91
Loma Prieta, CA, 1989/10/17 Saratoga Aloha Ave	LPsrtg	1.08
Loma Prieta, CA, 1989/10/17 Corralitos	LPcor	1.55
Loma Prieta, CA, 1989/10/17 Lexington Dam	LPllex1	1.60
Kobe, Japan, 1995/1/17 Kobe JM A	KBkobj	2.06
Tottori, Japan, 2000/10/6 Hino	TOhino	2.19
Erzincan, Turkey, 1992/3/13 Erzincan	EZerzi	2.60



Scaled response spectra for the 10 ground motions used in this study together with their average spectrum and the IBC2000 spectrum for a site located on Soil Type C in downtown Berkeley, CA

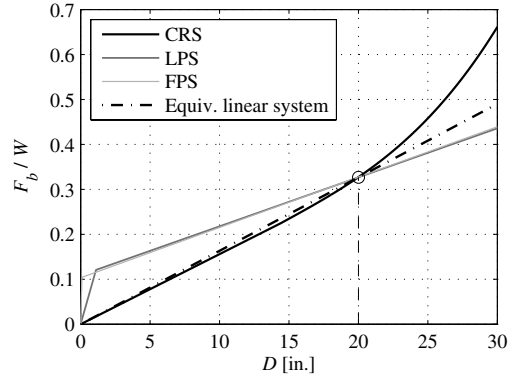


Figure 2. Load-displacement behaviour of the different isolation systems and the equivalent linear system

6. DESIGN OF FRICTION PENDULUM SYSTEM

In the case of the FPS, K_1 is selected as $100K_2$. Starting with the design displacement of 20.0 in. at the MCE hazard level (with 20% damping), the properties of the FPS are obtained using the aforementioned iterative procedure,

$$Q = 0.103W; \quad K_2 = 0.0112W; \quad D_y = 0.0932 \text{ in.} \quad (6.1)$$

at the MCE hazard level. The load-displacement curve for the FPS is shown in Fig. 2. When the hazard is reduced to DBE level (i.e., $S_{D1} = 2S_{M1}/3 = 0.82$), the system converges to a displacement of 10.4 in., a damping ratio of 29.6%, and an effective period of 2.20 sec. The further reduction of the input to the SLE level (i.e., $S_{S1} = S_{M1}/3 = 0.41$), the system converges to a displacement of 3.08 in., a damping ratio of 46.2% and a period of 1.51 sec. At these levels of damping and stiffness, the system can hardly be considered to be an isolation system.

7. DESIGN OF SYSTEM WITH CRYSTALLIZING RUBBER

In this section, we will discuss the details of a natural rubber bearing system that up to a certain level of displacement is linear with low damping. The intent is to design a system that will permit full isolation for sensitive internal equipment at moderate levels of seismic input. The control of displacements at high levels of input is to be achieved by exploiting a property of natural rubber known as strain-induced crystallization. This phenomenon has been known for a long time (Flory 1947) and has been extensively studied for the behaviour of thin sheets of rubber in tension. It is the reason for the inherent toughness of rubber in tension. It has been less well studied for rubber in shear, but most natural rubber compounds will crystallize at some level of shear strain depending on the compounding and the amount of filler; it can range from 100% or higher but all natural rubber compounds will show the beginning of crystallization for shear strains around 200% (see for example Kelly 1991). Figure 3 shows typical hysteretic loops of an Andre (Silvertown UK Ltd.) natural (crystallizing) rubber bearing tested to 110% shear strain (left) and 222% shear strain (right). The bearing exhibits a linear elastic behaviour up to approximately 12 in. of displacement, after which it stiffens up. It should be noted that the compound used in the LPS bearings is selected by manufacturers so as not to stiffen at displacements smaller than those corresponding to the MCE level (Kasalanati and Dickson 2004).

While it is possible to develop natural rubber compounds that have essentially no damping in the linear range, it is actually easier to use compounds that have moderate levels of damping, e.g., equivalent linear viscous damping around 5% to 8%. For example, the equivalent linear viscous damping ratio of the CRS in Fig. 3 is 8.6% at 110% shear strain (left) and 8.4% at 222% shear strain (right). Lower or higher amounts of damping can be obtained by modifying the rubber compound. In

the analysis presented in this paper, 5% linear viscous damping is assumed. Another aspect of this crystallization process is that, in addition to stiffening, it leads to a large increase in energy dissipation in the rubber. This can be seen on the right of Fig. 3 where the hysteretic loops become fatter once the rubber starts to stiffen. In the design process, the data from tests can be used to generate stress-strain curves to provide a system with target displacements similar to those of the hysteretic examples of the previous section.

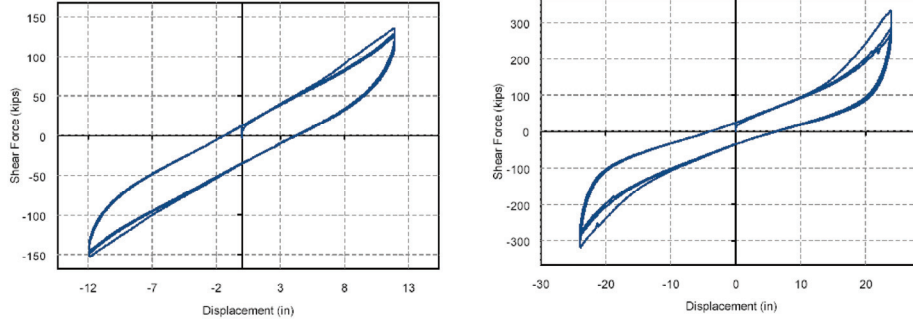


Figure 3. Hysteretic loops of typical CRS tested at 110% shear strain (left) and 222% shear strain (right)

To demonstrate the alternative approach of controlling the displacements by using the crystallization of the rubber, we begin with the premise that the problem faced by the designer is that the entirely linear system with 2.50 sec period has a code MCE displacement of 30.0 in. Data from a low-damping crystallizing rubber compound, tested at the Earthquake Engineering Research Center (EERC), UC Berkeley (Kelly and Quiroz 1990), was used to fit the force-deformation hysteresis response of the isolation system. The system behaves linearly up to $D \leq 3.5$ in with a initial stiffness of $K_H = 15.9$ kips/in. Beyond this,

$$F = \text{sgn}(D) \left(-39.34 + 46.09D \text{sgn}(D) - 8.026D^2 + 0.7450D^3 \text{sgn}(D) \right) \quad (7.1)$$

where F is in kips and D is in inches. This is converted to stress and strain using $\tau = F/A$ and $\gamma = D/t_r$, where A is the bearing area, and t_r is the total thickness of rubber. Using the values for the bearings tested, we have

$$\tau = \begin{cases} 90.4\gamma, & \gamma < 1.2 \\ -74.40 + 261.6\gamma - 136.6\gamma^2 + 38.00\gamma^3, & \gamma \geq 1.2 \end{cases} \quad (7.2)$$

in units of psi. As in the LPS and FPS systems, we assume that the three input levels for the design are $S_{M1} = 1.23$, $S_{D1} = 0.82$, $S_{S1} = 0.41$. The target displacements of the completely linear system with a period of 2.50 sec are $D_M = 30.0$ in., $D_D = 20.0$ in., and $D_S = 10.0$ in. The strategy is now to choose a Crystallizing Rubber System (CRS) design for which the material remains linear under SLE level deformations and linear or only slightly nonlinear under DBE deformations and considerably nonlinear (stiffer) under MCE deformations. For the analyses presented in this paper, an isolation system with $t_r = 12$ in. was selected. Since a period of $T_D = 2.50$ sec is desired at DBE, the effective stiffness of the isolation is $K_{\text{eff}} = (W/g)(2\pi/T_D)^2 = 0.0164W/\text{in}$. With $\beta_{\text{eff}} = 5\%$, the DBE displacement, D_D , from Eqn. (2.2) is 20.0 in., and the shear strain is $\gamma_D = D_D/t_r = 1.67$. Thus, from Eqn. (7.2), $\tau = 158$ psi, and the corresponding effective shear modulus is $G_{\text{eff},D} = \tau/\gamma = 94.8$ psi, which is only slightly larger than the linear elastic shear modulus of $G = 90.4$ psi; therefore, at the DBE displacement, the material is only slightly nonlinear.

The MCE displacement for the CRS is obtained by iteration on Eqn. (2.1) with $S_{M1} = 1.23$ and $B_M = 1$, which gives $D_M = 27.3$ in. The corresponding period is $T_M = 2.27$ sec. At the MCE design displacement, $\gamma_M = D_M/t_r = 2.28$, and $G_{\text{eff},M} = 114.8$ psi, which means that the material has stiffened considerably. When the material remains linear elastic, the period of the isolation system is $T_D \sqrt{G_{\text{eff},D}/G} = 2.56$ sec, and the stiffness of the isolation is $0.0156W$. When the material behaves

nonlinearly, the effective stiffness of the isolation system is given by $K_{eff} = 0.0156(G_{eff}/G)W/\text{in}$. Therefore, from Eqn. (7.2), the force in the isolation system as a fraction of the weight is

$$\frac{F_b}{W} = \begin{cases} 0.0156D, & D < 14.4\text{in.} \\ -\text{sgn}(D)(0.154 + 0.00196D^2) + D(0.0451 + 0.0000455D^2), & D \geq 14.4\text{in.} \end{cases} \quad (7.3)$$

where D is in inches. The force-displacement curve for the CRS is shown in Fig. 2. At the SLE level, the system is linear, and therefore no iteration is required to obtain the displacement. With $S_{S1} = 0.41$, $T_s = 2.56$ sec and $B_s = 1$, the SLE displacement is $D_s = (g/4\pi^2)(S_{D1}T_D/B_D) = 10.2$ in.

8. DYNAMIC ANALYSIS PROCEDURE

To examine the effect of the different isolation systems on the performance of the structure and equipment, a series of nonlinear dynamic analyses were conducted. Figure 4 shows the two-mass structural model used in this study. The mass m and m_b represent the mass of superstructure and the base floor mass above the isolation system, respectively. The structure stiffness and damping are represented by k_s and c_s and, if present, viscous damping in the isolation by c_b . The shear force in the isolator is denoted by F_b . For the LPS and the FPS, the F_b is calculated using the properties shown in Eqn. (5.1) and (6.1), respectively. For the CRS, the F_b is calculated using Eqn. (7.3). For comparison purpose, the F_b as a function of the isolator displacement is shown Fig. 2. The absolute displacements of the two masses are denoted by u_b and u_s , but it is convenient to use relative displacements, $v_b = u_b - u_g$ and $v_s = u_s - u_b$, where u_g is the ground displacement. This choice of relative displacements is particularly convenient for this analysis because the two important results will be the isolation system displacement, v_b , and the interstory drift, v_s . The equations of motion for the system are shown on the right of Fig. 4. Note that c_b is zero for all systems except the CRS, for which $\beta_b = c_b/2(m + m_b)\omega_b = 0.05$, with $\omega_b = \sqrt{k_b/(m + m_b)}$ defined at the linear part of the CRS (i.e., $k_b = 0.0156W/\text{in.}$). With $\lambda = m/(m + m_b) = 0.6$, $\beta_s = c_s/2m\omega_s = 0.02$, for all systems, $\omega_s = \sqrt{k_s/m}$, the equations of motion can be written in matrix form

$$\begin{bmatrix} 1 & \lambda \\ 1 & 1 \end{bmatrix} \begin{bmatrix} \ddot{v}_b \\ \ddot{v}_s \end{bmatrix} + \begin{bmatrix} 2\beta_b\omega_b & 0 \\ 0 & 2\beta_s\omega_s \end{bmatrix} \begin{bmatrix} \dot{v}_b \\ \dot{v}_s \end{bmatrix} + \begin{bmatrix} 0 & 0 \\ 0 & \omega_s^2 \end{bmatrix} \begin{bmatrix} v_b \\ v_s \end{bmatrix} + \begin{pmatrix} (F_b/W)g \\ 0 \end{pmatrix} = - \begin{bmatrix} 1 & \lambda \\ 1 & 1 \end{bmatrix} \begin{bmatrix} \ddot{u}_g \\ 0 \end{bmatrix} \quad (8.1)$$

More information on the model and time integration of Eqn. (8.1) is offered in Yang et al. (2010).

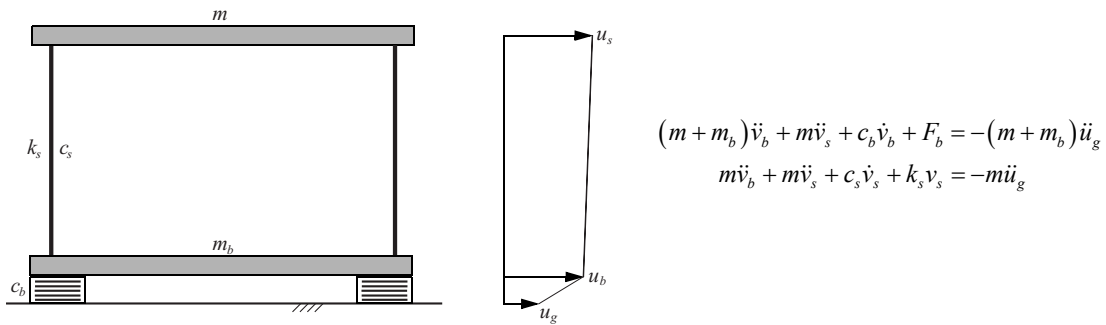


Figure 4. Two-degree-of-freedom isolated system its equations of motion

9. EFFECT OF ISOLATION TYPE ON STRUCTURAL AND EQUIPMENT PERFORMANCE

Table 3 shows the main results of the dynamic analyses: the mean of the maximum base-shear coefficients, isolator displacements and superstructure displacements using different isolation systems (FPS, LPS and CRS) at different earthquake shaking intensities (SLE, DBE and MCE) and with

different superstructure periods ($T_s = 0.10, 0.25, \text{ and } 0.50 \text{ sec}$). The results show that as the superstructure becomes more flexible, the displacement of the superstructure increases, but the displacement of the isolator and base-shear coefficients are almost unaffected. This shows that the displacement of the isolation system is almost independent of the superstructure period, and therefore its properties can be designed without regard of the superstructure's characteristics. Comparing with the results presented in Table 4, which lists the corresponding values for isolation displacement and base-shear coefficient as predicted by the code, the iterative procedure which uses the first-mode approximation provides a good estimate to the nonlinear response of the isolator.

Table 3. Mean of maximum responses recorded during the time history analyses

		SLE			DBE			MCE		
		FPS	LPS	CRS	FPS	LPS	CRS	FPS	LPS	CRS
$T_s=0.1s$	v_s [in.]	0.018	0.016	0.013	0.025	0.022	0.026	0.033	0.029	0.045
	v_b [in.]	3.4	4.9	8.1	9.4	10.5	16.1	16.4	17.3	23.6
	F_b/W	0.14	0.16	0.13	0.20	0.22	0.26	0.28	0.29	0.46
$T_s=0.25s$	v_s [in.]	0.18	0.12	0.08	0.23	0.17	0.16	0.26	0.22	0.28
	v_b [in.]	3.4	4.9	8.1	9.4	10.5	16.1	16.3	17.3	23.5
	F_b/W	0.14	0.16	0.13	0.20	0.22	0.26	0.28	0.29	0.45
$T_s=0.5s$	v_s [in.]	0.72	0.64	0.33	0.88	0.86	0.68	1.12	1.05	1.19
	v_b [in.]	3.6	5.0	8.0	9.6	10.6	16.0	16.2	17.0	23.2
	F_b/W	0.14	0.16	0.13	0.21	0.22	0.26	0.28	0.29	0.44

Table 4. Response quantities predicted by the code

	SLE			DBE			MCE		
	FPS	LPS	CRS	FPS	LPS	CRS	FPS	LPS	CRS
D_D [in.]	3.1	3.6	10.2	10.4	10.6	20.0	20.0	20.0	27.3
F_b/W	0.14	0.15	0.16	0.22	0.23	0.33	0.33	0.33	0.54

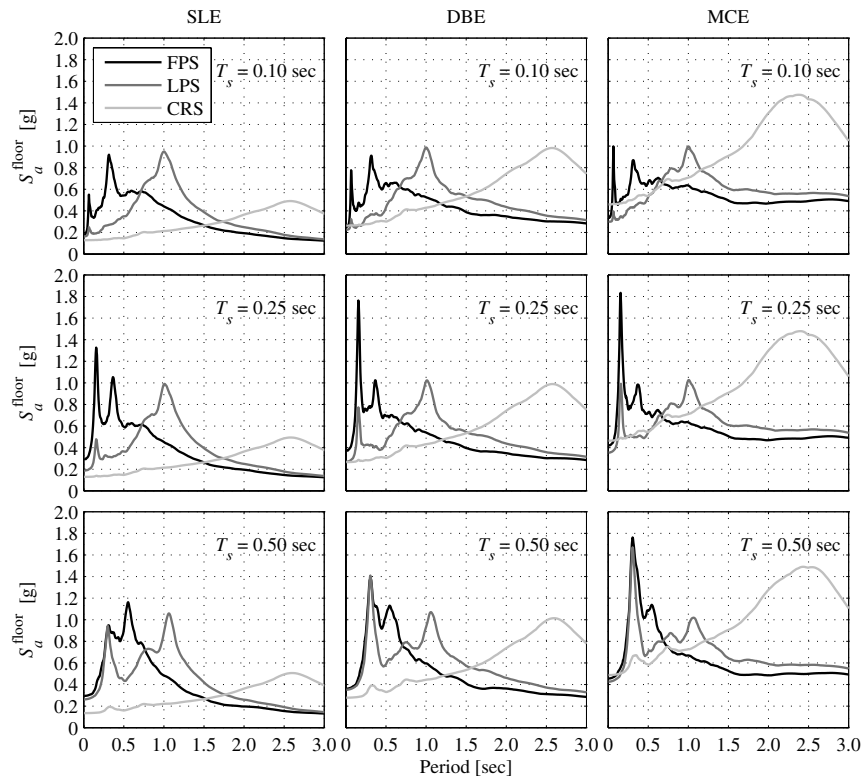


Figure 5. Mean floor acceleration spectra for the three isolation designs at the three hazard levels

Because the focus of this paper is to examine the performance of the equipment in the base-isolated building, the floor spectra (the response spectra due to the absolute floor acceleration $\ddot{u}_g + \ddot{v}_b + \ddot{v}_s$), the most direct design tool for attached equipment, was constructed. Figure 5 shows the mean floor spectra calculated from the ten time history analyses for the three seismic hazard levels and for the three types of isolation systems. The three rows of plots correspond to superstructure period, T_s , of 0.10, 0.25, and 0.50 sec, respectively. Overall, the FPS and LPS have higher floor spectra at the shorter period range, while the CRS has higher floor spectra at the longer period range. We note that although the CRS floor spectra attain large values at large periods, this is not a cause for concern for typical anchored equipment, whose natural period is substantially shorter (say, $T < 0.5$ sec).

In general, the floor spectrum for the FPS and LPS has two peaks (which were excited by the drastic changes in the stiffness of the isolators), while the CRS has only one distinct peak in the floor spectrum. As the period of the superstructure increases, the two peaks of the FPS floor spectrum and the lower-period peak of the LPS floor spectrum shift to longer periods (the longer-period peak of the LPS does not shift), while the peak of the CRS floor spectrum stays at approximately the same period. Overall, the floor spectrum for the FPS and LPS at long period does not depend on the flexibility of the superstructure. However, as the flexibility of the superstructure increases, the amplitude of the floor spectrum (for the FPS and LPS) at short periods increases drastically. It should be noted, that the peak spectrum acceleration at a few distinct periods might be additionally amplified by the resonance effect (very close fundamental periods) between the equipment and the superstructure. For the purpose of evaluating the performance of a range of short-period equipment, the results show that if the building is equipped with LPS or FPS, the equipment will be more vulnerable to the earthquake shaking as the flexibility of the superstructure increases. On the other hand, the floor spectrum for the CRS seems independent of the superstructure period for all periods in the range of interest. This means that it will be more advantageous to use the CRS to isolate buildings with sensitive equipment.

As the shaking intensity increases, the floor spectrum for the CRS increases almost linearly with ground motion amplitude. On the other hand, the amplitude of the peak floor spectrum for the FPS and LPS at longer period does not increase significantly, while the peak of the floor spectrum for the FPS and LPS at short period increases as the shaking intensity increases. This effect is further amplified as the superstructure period increases. This suggests that the peaks of the floor spectra for the LPS and FPS at longer period are limited by the characteristic strength of the isolator, while the peaks of the floor spectra for the LPS and FPS at shorter period are affected by the amplitude of the ground motion. The effect of the characteristic strength of the bilinear isolators is examined in Yang et al (2010).

Another useful observation from the mean floor spectra (Fig. 5) is that the CRS has the lowest floor spectra at the period range of interest for equipment ($T < 0.5$ sec), and its peak floor spectral acceleration is always less than 1.5 times the peak floor acceleration. On the other hand, the FPS has the highest floor acceleration, and in some cases it can be as high as 4.5 times the peak floor acceleration, showing that the CRS provides the best protection for equipment.

10. CONCLUSIONS

In this paper, the effect of different isolation systems on the structural and equipment performance was studied. This paper reviews the iterative procedure to design two commonly used isolation systems (LPS and FPS) in the US. Both of these systems have a bilinear hysteresis, where the parameters of the hysteresis were selected to ensure the isolation system could accommodate the earthquake shaking at the MCE hazard level. Due to the nature of these bilinear systems, as the isolator displacement decreases, the effective damping and stiffness of the isolation system increases. As a consequence, the efficiency of the isolation is decreased, leading to higher story drifts and floor vibrations.

To overcome these disadvantages, the authors have proposed a CRS which behaves essentially linearly elastic and has low viscous damping at lower and moderate shaking intensities (SLE and DBE). As the shaking intensity increases, the CRS will stiffen (due to strain-induced crystallization in the natural rubber), which will lower the isolation displacement. With the combination of these advantages, the

authors believe the CRS will be an efficient isolation system to protect both the equipment and structural components of the building at all hazard levels.

To demonstrate the above findings, three isolation systems were designed to comply with US building code requirements (ICC 2000), and a series of 270 nonlinear dynamic analyses were conducted to compare the dynamic response of the systems. The nonlinear dynamic analyses were carried out for three isolation types (FPS, LPS and CRS) with three superstructure periods ($T_s = 0.10, 0.25$ and 0.50 sec) and three hazard levels (SLE, DBE and MCE).

The results show that the displacement of the isolator and the base-shear coefficients are almost independent of the superstructure period. This suggests that the properties of the isolators can be selected without considering the design characteristics of the superstructure. However, if the purpose of the isolation is to protect acceleration-sensitive equipment, the flexibility of the superstructure plays an important role. In general, if the structure is base-isolated using FPS or LPS, the floor spectra at the short-period range increase as the superstructure period increases. On the contrary, the CRS has floor spectra that are almost independent of the superstructure period. In general, the CRS has the lowest floor spectra at the short period range that is of interest, and the peak floor spectrum is always less than 1.5 times the peak floor acceleration for $T < 0.5$ sec.

Although seismic isolation is a mature technology, only a few projects each year are initiated in the US; these are generally state, county, or city projects. In contrast, Japan and China design and build many isolated projects each year, with a high proportion of them being multi-family housing and commercial. In the US seismic isolation is perceived as expensive, complicated, and time-consuming. While these criticisms are valid for many recent projects in which isolation has been used, the fault lies not with the technology, but with the degree of over-regulation associated with the technology.

The benefits of seismic isolation in earthquake-resistant design are many: isolation leads to a simpler structure with much less complicated seismic analysis as compared with conventional structures; isolated designs are less sensitive to uncertainties in ground motion; and, finally, the components are much more reliable than conventional structural components. The drawbacks to using isolation stem directly from code documents that require the designer to use significantly larger factors of safety and, despite the availability of extensive test results on full-sized isolators of various types, testing of isolators is required for each project, ultimately hindering the widespread use of this technology.

REFERENCES

- ICC (2000). International Building Code 2000, International Code Council, Falls Church, VA.
- Flory P.J. (1947). The thermodynamics of crystallization in high polymers. I. Crystallization induced by stretching. *Journal of Chemical Physics* **15**: 397-408.
- Kasalanati A. and Dickson D. (2004). A study on the limit state performance of elastomeric isolators, JSSI 10th Anniversary Symposium on Performance of Response Controlled Buildings, Nov 2004, Yokohama, Japan.
- Kelly J.M. (1991). Dynamic and Failure Characteristics of Bridgestone Bearings, *Report No. UCB/EERC-91-04*, Earthquake Engineering Research Center, University of California, Berkeley, CA.
- Kelly J.M. and Quiroz E. (1990). Testing and Evaluation of CEGB Isolation System, *Report No. EERC Report 90-004*, Earthquake Engineering Research Center, University of California, Berkeley, CA.
- Marriott D., Pampanin S., Bull D., and Palermo A. (2008). Dynamic testing of precast, post-tensioned rocking wall systems with alternative dissipation solutions, *Bulletin of the New Zealand Society for Earthquake Engineering* **41**: 90-103.
- Mayer R.L. (2002). Impediments to the implementation of seismic isolation, *ATC-17-2 Seminar on Response Modification Technologies for Performance-Based Seismic Design*, May 30-31, 2002, Los Angeles, CA.
- Naaseh S., Morgan T.A., and Walters M.T. (2004). Future direction for base isolation design provisions, 2004 SEAOC Convention: 75th Anniversary Celebration, August 25-28, 2004, Monterey, CA.
- Skinner R.I., Robinson W.H., and McVerry G.H. (1993). *An Introduction to Seismic Isolation*, Wiley, Chichester, England.
- Yang T.Y., Konstantinidis D., and Kelly J.M. (2010) The influence of isolator hysteresis on equipment performance in seismic isolated buildings. *Earthquake Spectra* **26**(1), pp. 275-293.